

## COMPARATIVE PERFORMANCE STUDY OF MAGNETO-RHEOLOGICAL FLUID BASED DAMPER FOR VEHICLE SUSPENSION

A. S. M. Shawkatul Islam<sup>1</sup> and A. K. W. Ahmed<sup>2</sup>

<sup>1</sup> CONCAVE Research Centre, Concordia University, Montreal, Canada

<sup>2</sup> Dept. of Mechanical & Industrial Engineering, Concordia University, Montreal, Canada

### ABSTRACT

Magneto-Rheological (MR) fluid based suspension dampers have gained wide spread attention in academia as well as in auto industries due to their attractive features and promising performance potential to overcome the limitations of existing dampers in market. This study investigates the performance of MR damper by comparing with linear passive and asymmetric non-linear damper. Performance measures considered for this investigation are - sprung and unsprung mass responses, relative motion, load transfer ratio and ride height drift. The study reveals superior vibration isolation performance of MR damper for vehicle sprung mass compared to linear passive and asymmetric non-linear damper. Due to symmetric characteristics, MR damper exhibits no drift in the responses. At higher frequencies, the damper transmits higher load to pavement compared to other two. The study suggests that asymmetry should be included in the MR damper design to achieve improved performance over the entire frequency range.

**Keywords:** Suspension damper, Magneto-Rheological (MR) damper.

### 1. INTRODUCTION

Vehicle system ride and handling performances impose conflicting requirement on the design and properties of suspension system. Since selection of suspension spring parameter is restricted by desired low natural frequency of sprung mass, all the attention is directed to the damper design and its characteristics. To overcome the performance limitation of linear passive dampers, modern dampers used in vehicles are designed as asymmetric non-linear in compression and rebound. Asymmetric dampers can range from single stage to multi-stage depending on application. The asymmetry and the non-linear characteristic of these dampers work in a passive manner and must be designed for optimal performance under some operating conditions. In the past many researchers have proposed a number of semi-active concepts to achieve damping characteristics in an adaptive manner, with some success [1].

In the past decade, a new concept on 'Smart Fluid' based Magneto-Rheological (MR) suspension damper has gained widespread attention for its attractive features and performance potential to overcome the performance limitation of existing dampers. A MR based smart fluid is defined as one in which the resistance to flow can be controlled through the application of a magnetic field. In general, MR fluid consists of dispersions composed of meso-scale (1–10  $\mu\text{m}$ ) ferromagnetic or ferrimagnetic particulates dispersed in organic or aqueous carrier liquid [2]. A typical MR fluid consists of 20-40% by volume of

relatively pure soft iron particle, suspended in carried liquid like mineral oil, synthesis oil, water or a glycol [3]. The MR fluid particles form chain-like fibrous structures in the presence of magnetic field. When the magnetic field strength reaches a certain value, the fluid suspension will be solidified and has high yield stress. Conversely, the suspension can be liquefied by removal of the magnetic field. The process of change is very quick, and takes less than few milliseconds, and can be easily controlled [4]. Fig 1 shows the response of MR fluid to applied magnetic field.

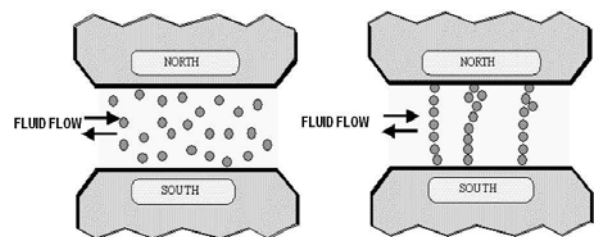


Fig 1. Response of MR fluid to applied magnetic field [5]

In the past few years various studies have focused on MR fluid based damper technology. MR damper equipped with Linear Quadratic (LQ) control has shown improved ride comfort in the frequency range of 4 to 8 Hz [6]. Industry developed MR damper such as MR 132-LD from Lord Corporation can effectively control

acceleration response of sprung mass, suspension travel, and tire deflection around the body resonance [7]. MR dampers can be used effectively as seat suspension. The damper improves vibration isolation by providing high damping force when the seat displacement approached the end limits of the free travel of the suspension, and lower damping closer to mid-ride [5].

Semi-active skyhook control is widely used to control the damping force of such dampers. Studies have suggested that skyhook model could yield superior vibration isolation performance of the MR-damper when considered in conjunction with a quarter-vehicle model as well as full vehicle model [7, 8, 9].

In spite of few unfavorable conditions for automotive applications, MR fluid based damper system was produced for 2002 Cadillac Seville STS [10]. The fluid used in the damper can respond within 1ms resulting in a 5 time faster reaction than previous passive systems.

Although few studies investigate comparative performance of MR damper with linear damper, there is a lack of comparative study involving MR damper and asymmetric non-linear damper. Since asymmetric dampers are commonly used in road vehicles, it is very important to compare the performance of MR damper with asymmetric damper to reflect on the possibility of MR damper as substitute of asymmetric damper. This study compares the vibration isolation performance of MR damper with a linear passive damper and a two stage non-linear asymmetric damper. The damper models are described in the following section.

## 2. SUSPENSION DAMPER MODELS

The two degree-of-freedom (DOF) quarter-car model, shown in fig 2, is commonly utilized to evaluate sprung and unsprung mass bounce characteristics and dynamic rattle space requirements of road vehicles.

The performance of the candidate dampers of this study are compared using 2 DOF quarter car model.

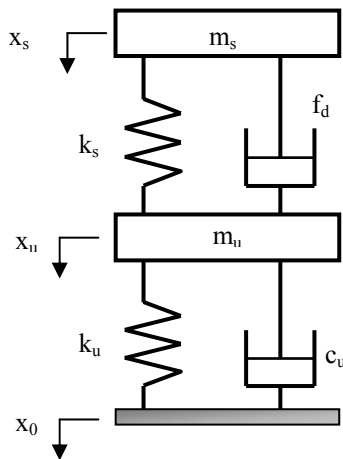


Fig 2. Quarter car model

The equation of motion of the quarter car model can be written as:

$$m_s \ddot{x}_s + f_d + k_s (x_s - x_u) = 0 \quad (1)$$

$$m_u \ddot{x}_u - f_d + c_u (\dot{x}_u - \dot{x}_0) - k_s (x_s - x_u) + k_u (x_u - x_0) = 0 \quad (2)$$

where,  $m_s$ (=231 kg),  $m_u$ (=17 kg),  $k_s$ (=12,800 N/m),  $f_d$ ,  $k_u$ (=150,000 N/m) and  $c_u$ (= 750N/m) represents one quarter sprung mass of the vehicle, unsprung mass associated with one tire of the vehicle, suspension spring stiffness for one suspension, damping force of one damper, tire stiffness coefficient and tire damping coefficient respectively. The values of the parameters are typical of those used for a small-size passenger car.  $x_s$ ,  $x_u$ ,  $x_0$  represents the sprung mass displacement, unsprung mass displacement, road input to one tire of the vehicle, respectively.

The term  $f_d$  used to represent the suspension damping force in equations 1 and 2 are not defined.  $f_d$  depends on the type of suspension damper used and is discussed in the following subsections.

### 2.1 Linear Passive Damper

Linear passive damper provides constant damping force throughout the operating cycle of the damper. The damping force of such a damper is expressed as product of a damping constant ( $c_s$ ) and relative velocity across the damper ( $\dot{x}$ ). For this study, the suspension damping coefficient for the linear passive damper is based on a damping ratio of 15%. The linear damper is used as bench mark to compare the performance of the other two.

### 2.2 Two Stage Asymmetric Damper

The suspension dampers used in modern vehicles are more sophisticated than the linear passive damper. The dampers used in today's vehicles are designed to yield variable and asymmetric damping characteristics to achieve improved ride and handling performance. The dynamic force developed by such modern hydraulic dampers comprise of following major components: (a) hydraulic force attributed to pressure drop across the flow paths, such as orifices and valves; (b) restoring force due to gas spring; and (c) seal friction force. The magnitudes of the two latter components are considerably small compared to that of the hydraulic force. Thus the dampers are mainly characterized by their hydraulic force components, which are strongly non-linear function of the velocity. However, non-linear nature of these dampers poses considerable challenges associated with analytical modeling and performance analyses of the dampers. Owing to these complexities, the majority of the studies on vehicle ride analysis consider either linear or linear equivalent damping characteristics. Despite the fact that these analyses facilitate preliminary design analysis and exploration of different damping concepts, but neglects the effects of damping asymmetry and non-linear variations with the relative velocity. A few studies have characterized asymmetric damping properties of modern passive dampers by a piece-wise linear function [11, 12]. Fig 3 represents typical damping force-velocity ( $f$ - $v$ ) characteristics of a two-stage asymmetric damper.

The velocities ( $\alpha_c$ ,  $\alpha_e$ ), where the transitions from low speed damping coefficients ( $C_1$  and  $C_3$ ) to the high speed coefficients ( $C_3$  and  $C_4$ ) occur, can be identified from the measured data. The piece-wise linear describing function models has been effectively employed in ride dynamic models of different vehicles [11]. The piece-wise linear

representation is considered adequate to study the effects of damping asymmetry and non-linearity.

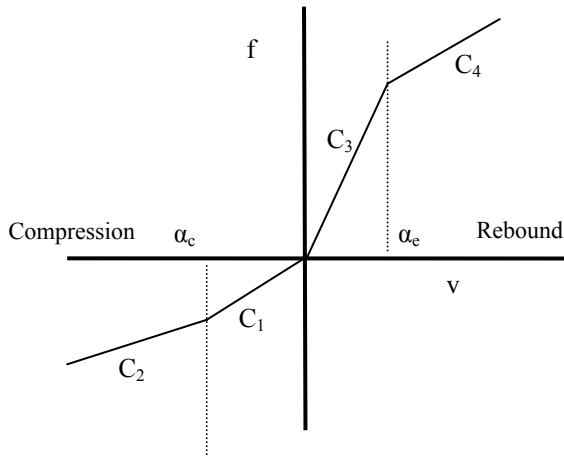


Fig 3.  $f$ - $v$  characteristics of two-stage asymmetric damper

Damping force generated by such damper can be expressed as:

$$f_d = \begin{cases} C_1 \dot{x}; & \text{for } \alpha_c \leq \dot{x} \leq 0 \\ C_1 \alpha_c + C_2 (\dot{x} - \alpha_c); & \text{for } \dot{x} \leq \alpha_c \\ C_3 \dot{x}; & \text{for } 0 \leq \dot{x} \leq \alpha_e \\ C_3 \alpha_e + C_4 (\dot{x} - \alpha_e); & \text{for } \dot{x} \geq \alpha_e \end{cases} \quad (3)$$

where,  $f_d$  represents the damping force generated by the damper and  $C_1, C_2, C_3, C_4$  represent high damping coefficient at compression side, low damping coefficient at compression side, high damping coefficient in the extension side and low damping coefficient in the extension side respectively.  $\alpha_e$  and  $\alpha_c$  are the preset velocities at compression and extension side respectively and  $\dot{x}$  represents the velocity of the damper piston (relative velocity across the damper). The values of the parameters are adopted from [11].

### 2.3 Magneto-Rheological (MR) Fluid Damper

Magneto-Rheological (MR) fluid based semi-active damper operates based on alteration of fluid viscosity depending on an applied magnetic field. Lord Corporation, USA is the leading manufacturer of MR dampers. For this study, a cylindrical type MR damper model RD-1005-3, manufactured by Lord Corporation, is selected for the analysis of the characteristics of MR type damper. The damper is shown in fig 4. The damper consists of a nitrogen-charged accumulator, which is located at the bottom of the damper. The two MR fluid chambers are separated by virtue of a piston. A number of coils are located within the piston and annular orifice area, which generates magnetic field for the fluid. Under the application of magnetic field, variations in viscous and shear properties of the fluid occurs, which eventually yields variations in the damping force developed by the damper. The damper was tested in CONCAVE Research Centre of Concordia University under different operating conditions.

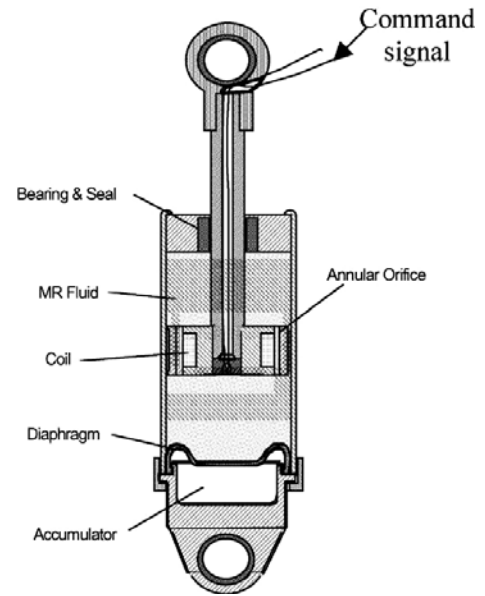


Fig 4. Schematic diagram of MR damper [13]

Based on the experimental data the damping force generated by the MR damper can be expressed in the following manner [13]:

$$f_d = f_t(i) \frac{1 - e^{-\alpha(v \pm v_h)}}{\{1 + e^{-\alpha(v \pm v_h)}\} (1 + k_v \cdot |v|)} \quad (4)$$

where,  $f_d$  denotes the damping force as a function of the control current ( $i$ ) and piston velocity ( $v$ ), and  $v_h$  is the piston velocity corresponding to zero damping force, given by:

$$v_h = \text{sign}(\ddot{x}) k_4 v_m [1 + \{k_3 / 1 + e^{-a_3 \cdot (i + I_1)}\} - (k_3 / 1 + e^{-a_3 \cdot I_1})] \quad (5)$$

$f_t$  is transition force, which depends upon  $i$  and the peak velocity  $v_m$ , given by:

$$f_t(i) = f_0 \cdot (1 + e^{a_1 \cdot v_m}) [1 + \{k_2 / 1 + e^{-a_2 \cdot (i + I_0)}\} - (k_2 / 1 + e^{-a_2 \cdot I_0})] \quad (6)$$

The parameters  $k_v$  and  $\alpha$  in equation 4 is used to adjust the damping coefficients at high and low velocities respectively, are expressed as functions of the peak velocity  $v_m$ , and are given by :

$$k_v = k_1 \cdot e^{-a_4 \cdot v_m} \quad (7)$$

$$\alpha = a_0 / (1 + k_0 \cdot v_m) \quad (8)$$

The damping force model presented in equation 4 requires identification of 13 parameters from the measured data, namely  $f_0, I_0, I_1, a_0, a_1, a_2, a_3, a_4, k_0, k_1, k_2, k_3, k_4$ . The values are adapted from [13]. The peak velocity parameter  $v_m$  can be estimated from the instantaneous displacement  $x$ , velocity  $\dot{x}$  ( $v = \dot{x}$ ), and acceleration  $\ddot{x}$  responses across the piston of the damper.

For harmonic excitations parameter  $v_m$  is obtained from the following equation:

$$v_m = a_m \cdot \omega = \sqrt{\{(\dot{x})^2 - \ddot{x} \cdot x\}} \quad (9)$$

where,  $a_m$  and  $\omega$  are excitation amplitude and frequency respectively.

MR fluid dampers are generally used as semi-active dampers. The most commonly used semi-active control strategy is ‘skyhook’ control, which is based on the ‘skyhook’ control law proposed by Karnopp *et al.* [14]. The control law suggests that the damper should be switched to high damping mode, when the absolute mass velocity is in phase with the damper relative velocity. Otherwise, the damper should be switched off. For the current study, skyhook control law based controller is used to control the damping force of the MR damper. The control scheme is presented in fig 5.

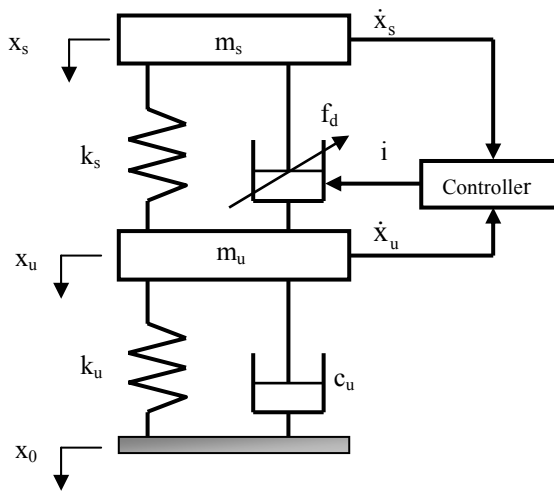


Fig 5. Schematic representation of the control scheme for MR damper

The ‘skyhook’ control synthesis is formulated to modulate the control current ( $i$ ) supply to the MR damper to control the damping force,  $f_d$ , in the following manner:

$$\begin{aligned} i &= C_{sky} |\dot{x}_s|; & \dot{x}_s \cdot (\dot{x}_s - \dot{x}_u) &\geq 0 \\ i &= 0; & \dot{x}_s \cdot (\dot{x}_s - \dot{x}_u) &< 0 \end{aligned} \quad 0 < i \leq i_{max} \quad (10)$$

where,  $C_{sky}$  is the adjustable gain of the ‘skyhook’ controller,  $\dot{x}_s$  and  $\dot{x}_u$  are the velocity of the sprung mass and unsprung mass respectively. The control current ( $i$ ) should be limited to a peak value depending on the coil design of the electro-magnet.

### 3. PERFORMANCE MEASURES

The performance measures considered for this study of a vehicle under sinusoidal input (in phase) are – sprung mass displacement transmissibility [ $X_s/X_0$ ], unsprung mass displacement transmissibility [ $X_u/X_0$ ] suspension travel ratio [ $(X_s - X_u)/X_0$ ], load transfer ratio and ride height drift (also known as packing down of suspension).

### 4. COMPARATIVE PERFORMANCE STUDY

The 2DOF quarter car model with each damper is simulated in time domain using MATLAB® SIMULINK. The vibration isolation performances of the dampers are compared at excitation amplitude of 10mm, which represents reasonable road input, over a wide sinusoidal frequency range. The frequency range of 0.5 to 18 Hz is considered appropriate for vehicle ride performance analysis. Several trial runs were carried out to establish damper parameters such that all dampers produces comparable performance for the vehicle parameters used over the entire frequency range. Details of the study and parameters can be found in [15].

The sprung mass displacement transmissibility ratios of the vehicle model using all the dampers are presented in fig 6. The results represent sprung mass transmissibility of the candidate dampers tuned such a way that they all produce similar ride quality for higher frequencies, while minimize the response at resonance (1.1Hz). A comparison of the three dampers clearly reveals the superiority of asymmetric damper over linear passive, and the effectiveness MR over the entire frequency range. It is also been observed that, at frequencies above the sprung mass natural frequency, the transmissibility values decrease more rapidly for MR damper compared to the asymmetric case.

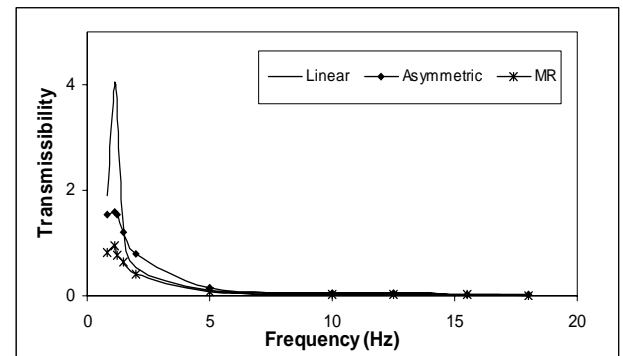


Fig 6. Sprung mass transmissibility of the dampers

The unsprung mass displacement transmissibility ratios of the vehicle model using all three dampers are presented in fig 7. The figure shows that, in the frequency range around the unsprung mass natural frequency (15.5 Hz), the transmissibility ratio is highest. It is evident from the results that, although MR damper provides better vibration isolation to sprung mass compared to linear and asymmetric, it provides poor isolation to unsprung mass. The MR dampers thus provide superior sprung mass transmissibility at the expense of performance for unsprung mass response.

An interesting aspect in the results shown in fig. 7 is the fact that asymmetric damper provides superior performance compared to linear, for both sprung and unsprung mass transmissibility over the entire frequency range, and better performance in terms of unsprung mass response compared to MR damper. This can be attributed to better road holding capability of asymmetric damper. Since the MR damper model is symmetric in compression and rebound, introduction of asymmetry in the damper might improve the unsprung mass

response of the damper.

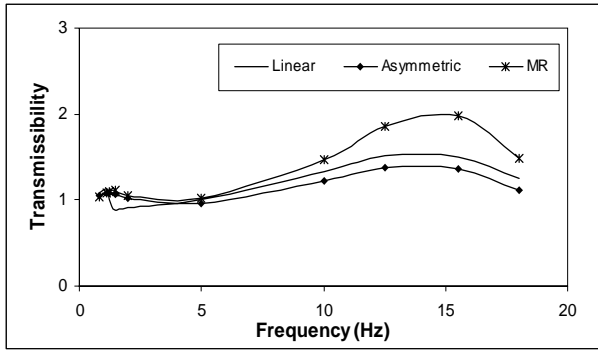


Fig 7. Unsprung mass transmissibility of the dampers

The suspension travel ratios for candidate dampers are presented in fig 8. The ratios are higher around natural frequencies for all the dampers. The results indicate MR damper requires low rattle space around sprung mass natural frequency, while around unsprung natural frequencies they require higher rattle space compared to linear and asymmetric damper.

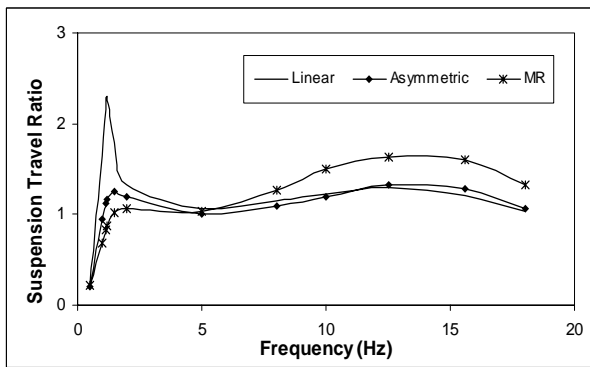


Fig 8. Suspension travel ratio of the dampers

All the candidate dampers show higher load transfer ratio around unsprung mass natural frequencies of the vehicle.

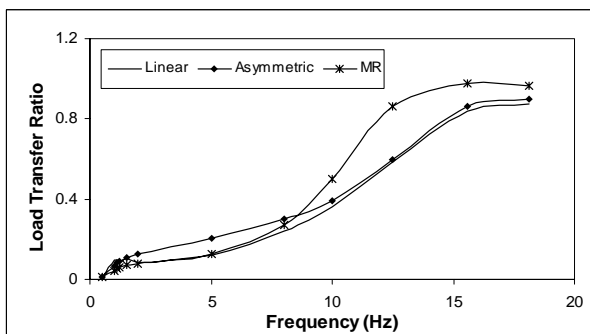


Fig 9. Load transfer ratio of the dampers

Fig 9 presents load transfer ratio for the candidate dampers. It is evident from the results that MR damper will cause more damage to road than linear and asymmetric damper. The higher pavement load results from low damping force generated by MR damper at

higher frequencies compared to linear and asymmetric damper.

Ride height drift is the shift of dynamic equilibrium of the sprung mass and is the direct result of asymmetric damping properties. Except asymmetric damper, linear and MR damper have symmetric f-v characteristics in compression and rebound. Hence it is expected that linear and MR damper will show no or negligible drift. The simulation results indicated that linear and MR damper model have either negligible drift or no drift at all. The ride height drifting problem is only seen in asymmetric damper. For asymmetric damper, the drift is low at lower frequencies and maximum around unsprung mass natural frequency. Fig 10 shows the ride height drift of asymmetric damper.

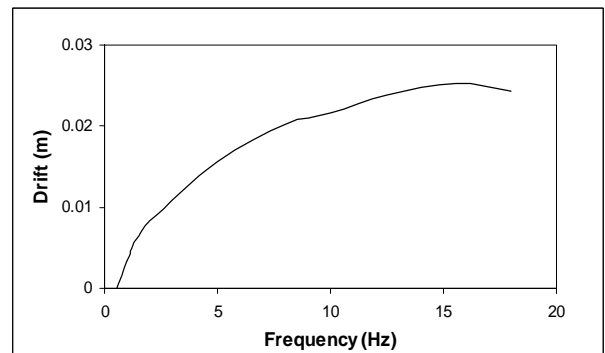


Fig 10. Ride height drift of asymmetric damper

## 5. CONCLUSIONS

The comparative study of three dampers clearly indicates that MR damper provides superior vibration isolation to sprung mass over entire frequency range compared to linear passive and asymmetric non-linear damper at the expense of unsprung mass performance. Rattle space required for MR damper is high around unsprung mass natural frequency compared to linear and asymmetric damper. Among all the dampers considered, the MR produces the largest pavement load as it is controlled to produce low damping at high frequencies. Due to symmetric characteristics, MR damper exhibits no drift in the responses.

The study reveals that asymmetricity is needed for suspension to perform better around unsprung mass natural frequency. Thus asymmetric properties should be included in the MR damper model to achieve improved performance for sprung and unsprung mass. It can be done by modifying the controllers for such damper to monitor the compression and rebound and change the gain accordingly.

## 6. REFERENCES

1. Ficher, D., Isermaan, R., 2004, "Mechatronic Semi-active and Active Vehicle Suspensions", Control Engineering Practice, 12: 1353-1367.
2. Genç, S., Phulé, P.P., 2002, "Rheological Properties of Magnetorheological Fluids", Smart Materials and Structures, 11 (1):140-146.
3. Carlson, J.D., 2000, "Implementation of Semi-Active Control Using Magneto-Rheological

Fluids”, *Mechatronic System: A Proceeding Volume from the IFAC Conference*, Darmstadt, Germany, pp. 905-910.

4. Sims, N. D., Peel, D. J., Stanway, R., Johnson, A. R., 1999, “Vibration Control Using Smart Fluids: A State-of-art Review”, *The Shock and Vibration Digest*, 31 (3): 195-203.
5. McManus, S. J. , Clair, K. A. ST., Boileau, P. É, Boutin, J., Rakheja, S., 2002, “Evaluation of Vibration and Shock Attenuation Performance of a Suspension Seat with a Semi-Active Fluid Damper”, *Journal of Sound and Vibration*, 253(1):313-327.
6. Kim, K., Lee, J., Jeon, D., 1999, “Vibration Suppression of an MR Fluid Damper System with Frequency Shaped LQ Control”, *Proc. of the 7<sup>th</sup> Int. Conf. on Electro-Rheological Fluids and Magneto-Rheological Suspensions*, Hawaii, USA, pp. 649-656.
7. Yao, G.Z., Yap, F.F., Chen, G., Li, W.H., Yeo, S.H., 2002, “MR Damper and Its Application for Semi-Active Control of Vehicle Suspension System”, *Mechatronics*, 12 (7):963-973.
8. Yokoyama, M., Hedrick, J.K., Toyama, S., 2001, “A Model Following Sliding Mode Controller for Semi-Active Suspension Systems with MR Dampers”, *Proc. of American Control Conf.*, pp. 2652-2657.
9. Lee, H.S., Choi, S.B., 2000, “Control Responses Characteristics of a Magneto-Rheological Fluid Damper for Passenger Vehicles”, *Journal of Intelligent Materials Systems and Structures*, 11(1): 80-87.
10. Gilbert, R., Jackson, M., 2002, *Magnetic Ride Control*, GM TechLink 4.
11. Rakheja, S., Ahmed, A. K. W., 1993, “Frequency Response Analysis of Symmetric and Asymmetric Nonlinear Vehicle Suspensions”, *CSME Special issue*, 17(4B), Canada.
12. Rajalingham, C., Rakheja, S., 2003, “Influence of Suspension Damper Nonlinearity on Vehicle Vibration Response of Ground Excitation”, *Journal of Sound and Vibration*, 266(5):1117–1129.
13. Ma, X.Q., Wang, E.R., Rakheja, S., Su, C.-Y. , 2002, “Modeling Hysteretic Characteristics of MR-Fluid Damper and Model Validation”, *Proc. of 41<sup>st</sup> Conf. on Decision and Control*, Las Vegas, Nevada, USA.
14. Karnopp, D.C., Crosby, M.J., Harwood, R.A., 1974, “Vibration Controlling Semi-Active Generators”, *ASME Journal of Engineering for Industries*, 96B (2): 619-626.
15. Islam, A.S.M.S., 2005, “A Comparative Study of Advanced Suspension Dampers for Vibration and Shock Isolation Performance”, M.A.Sc. thesis, Concordia University, Montreal, Canada.

## 7. NOMENCLATURE

Symbol	Meaning	Unit
$m_s$	Sprung mass	(kg)
$m_u$	Unsprung mass	(kg)
$k_s$	Suspension stiffness coefficient	(N/m)
$f_d$	Suspension damping force	(N)
$c_u$	Tire damping coefficient	(Ns/m)
$k_u$	Tire stiffness coefficient	(N/m)
$c_s$	Suspension damping coefficient (linear damper)	(Ns/m)
$C_1$	High damping coefficient at compression	(Ns/m)
$C_3$	High damping coefficient at extension	(Ns/m)
$C_2$	Low damping coefficient at compression	(Ns/m)
$C_4$	Low damping coefficient at extension	(Ns/m)
$\alpha_e$	Preset velocity at extension	(m/s)
$\alpha_c$	Preset velocity at compression	(m/s)
$v_m$	Maximum velocity	(m/s)
$f_m$	Maximum damping force	(kN)
$v_h$	Zero force velocity intercept	(m/s)
$f_h$	Zero velocity force intercept	(kN)
$v_t$	Transition velocity	(m/s)
$f_t$	Transition force	(kN)
$s_h$	Hysteretic slope	(m/s) <sup>-1</sup>
$a_m$	Excitation amplitude for MR damper	(m)
$\omega$	Excitation frequency for MR damper	(rad/s)
$a_0$	MR damper parameter	(None)
$a_1$	MR damper parameter	(m/s) <sup>-1</sup>
$a_2$	MR damper parameter	(amps) <sup>-1</sup>
$a_3$	MR damper parameter	(amps) <sup>-1</sup>
$a_4$	MR damper parameter	(m/s) <sup>-1</sup>
$I_0$	MR damper parameter	(amps) <sup>-1</sup>
$I_1$	MR damper parameter	(amps) <sup>-1</sup>
$k_0$	MR damper parameter	(None)
$k_1$	MR damper parameter	(None)
$k_2$	MR damper parameter	(None)
$k_3$	MR damper parameter	(None)
$k_4$	MR damper parameter	(None)
$f_0$	MR damper parameter	(N)
$C_{sky}$	Skyhook controller gain	(m/s) <sup>-1</sup>